Ecotoxicology and Environmental Safety 246 (2022) 114145

Contents lists available at ScienceDirect

Ecotoxicology and Environmental Safety

journal homepage: www.elsevier.com/locate/ecoenv

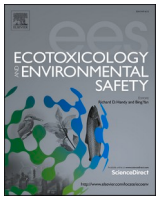

Emission and transformation behaviors of trace elements during combustion of Cd-rich coals from coal combustion related endemic fluorosis areas of Southwest, China

Yan Xiong [a], Zengping Ning [b], Yizhang Liu [b], Mario Gomez [c,d], Tangfu Xiao [c,d,*]

[a] College of Chemistry and Materials Engineering, Guiyang University, Guiyang 550005, China
[b] State Key Laboratory of Environmental Geochemistry, Institute of Geochemistry, Chinese Academy of Sciences, Guiyang 550081, China
[c] School of Environmental Science and Engineering, Guangzhou University, Guangzhou 510006, China
[d] Key Laboratory for Water Quality and Conservation of the Pearl River Delta, Ministry of Education, Guangzhou University, Guangzhou 510006, China

ARTICLE INFO

Edited by Dr G Liu

Keywords:
Trace element
Emission
Combustion
Cd-rich coal
Endemic fluorosis areas

ABSTRACT

Long-term combustion of low-quality coal may release hazardous elements into the environment causing serious environmental problems. This phenomenon is particularly prevalent in the Three Gorges Region of Southwest (SW), China. Cadmium (Cd), as well as other harmful elements are found to be highly enriched in coals and supergene environments in this area. In the existing literature, the behavioral issue of emission and transformation of the elevated trace elements during simulated household stove combustion from Cd-rich inferior coal remains unknown. This study investigated the emission of toxic elements, mineral assemblages, and provided technical guidance for reducing pollution by means of optimization combustion tests on inferior coals. The research may improve the understanding of geochemical characteristics from toxic elements emission in coal combustion endemic diseased areas. For this purpose, a series of simulated coal combustion experiments were conducted to reveal the release, mobility, and distribution of elevated elements in Cd-rich coal combustion products. The results showed that Cd, Mo, Cr, Cu, Zn, As, and Sb were significantly enriched in the inferior coals of the study area. Furthermore, large amounts of toxic elements were released as fly ash into the environment during the combustion process. In particular, combustion conditions played an important role in the emission and transformation of elevated elements. For example, higher temperatures promoted the release of Cd, Sb, Zn, and Tl into the environment. Oxygen-deficient combustion was found to liberate more Cd, Sb, and Tl to the atmosphere and generated complex mineral assemblages of lizardite, calcite, dolomite, forsterite, and enstatite. Moreover, toxic elements were found to be absorbed in the fine particle matter of fly ash from the endemic fluorosis area of SW, China. The findings of this work may aid to control the emission of toxic elements from inferior coals and mitigate the effect of toxic elements in the environment to protect human health.

1. Introduction

Coal is a type fossil fuel that is formed through a series of biochemical, physical, chemical, and geological processes (Bernard and William, 1984). Based on Chinese natural resource data, the explored coal reserves found in 2017 amounted to approximately 1683.31 billion tons (Ministry of Natural Resources of the People's Republic of China, 2018). Coal is one of the most important energy resources in China that accounts for approximately 67.6% of the primary energy consumption (Department of Energy Statistics of National Bureau of Statistics of China, 2021).

Due to the complex environmental conditions that take place when coal is formed, almost all elements in the periodic table may be present (Vejahati et al., 2010). Some of these elements may be particularly harmful to public health. The release and associated environmental risk that these trace elements exhibit during coal combustion processes are of great concern (Saikia et al., 2015; Zeng et al., 2018). The fast-growing coal consumption in China has produced a huge volume of toxic elements associated combustion. Such processes can therefore introduce considerable quantities of toxic elements such as fluorine (F), arsenic (As), antimony (Sb), zinc (Zn), cadmium (Cd), chromium (Cr), mercury (Hg), and molybdenum (Mo) to the environment through gas emissions

* Correspondence to: School of Environment Science and Engineering, Guangzhou University, Room 419, Guangzhou 510006, China.
E-mail address: tfxiao@gzhu.edu.cn (T. Xiao).

https://doi.org/10.1016/j.ecoenv.2022.114145
Received 18 July 2022; Received in revised form 23 September 2022; Accepted 29 September 2022
Available online 7 October 2022

(Bhangare et al., 2011; Dai et al., 2017; Deng et al., 2014; Dziok et al., 2019; Liu et al., 2010; Ma et al., 2021; Zhang et al., 2003). For example, gaseous emissions of F, As, Se, and Sb from coal combustion in China during 2009 were about 162,161 t, 236 t, 637 t, and 33 t, respectively (Chen et al., 2013). Meanwhile, the total emissions of Cd and Cr from coal burning in China have rapidly increased from 31.14 t and 1019.07 t in 1980–261.52 t and 8593.35 t in 2008 (Tian et al., 2012). Volatile elements are possibly emitted into the air or adsorbed onto fine particles through coal combustion, these can then be subsequently deposited onto aqueous and terrestrial systems by dry and wet deposition (Hay-kiri-Acma et al., 2011). In addition, coal mining activities produce large amounts of solid waste and acid mine drainage with high levels of toxic elements that can severely pollute the soil and water (Orndorff et al., 2015). These toxic elements persist in the environment and accumulate in the food chain causing adverse effects to human health.

The emission and transformation behavior of toxic elements during coal combustion varies in terms of the type of coal (i.e., grade) and locality. However, the main proportion of trace elements is bound to fly ash (Xu et al., 2003; Zhao et al., 2019). The primary causes that impact trace element emission during coal combustion are the form in which they occur, the minerals that carry the trace elements, the distribution of particle size found in the fly ash, the type of surface reactions, and chemisorption sites that exist in the active minerals (Seames and Wendt, 2000; Yi et al., 2008; Zhou et al., 2017). Furthermore, the type of cleaning technique and combustion conditions (e.g. temperature, oxygen, and retention time) also play an essential role in the partitioning of trace elements from coal combustion byproducts (Oboirien et al., 2014; Quick and Irons, 2002; Wang et al., 2009; Zhou et al., 2015).

Domestic coal combustion represents a major pathway of long-term environmental exposure from toxic elements to indoor human health. For example, local residents in rural areas of SW, China have suffered from coal-burning related endemic diseases such as chronic poisoning of F (Zheng et al., 2007) and As (Zheng et al., 2005). This is because coal was burned indoors for cooking and heating without proper ventilation. Previous work by Tang et al. (2009) noted that elevated Cd in coals from the Three Gorges region of SW, China represents an unrecognized toxin that may also pose an endemic problem. Other studies by Xiong et al. (2017) have further suggested that Cd, Mo, and other elements enriched in local coals and coal wastes may also pose health risks during weathering processes and surface enrichment. However, little is known with respect to the mobility and transport of trace elements that occur during coal combustion in this area. Thus, it is important to understand the release and transportation features of toxic metals in coal combustion processes to better control indoor air pollution. And in particular, occurrences of toxic elements in bottom slag, fly ash, and tail gas from indoor coal combustion of endemic fluorosis areas in SW, China should be investigated. Consequently, this paper is aimed at understanding the emission and transformation behaviors of toxic elements during coal combustion, as well as identifying mineralogical features of inferior coals from an endemic fluorosis area in SW, China. The findings of this work may be beneficial to environmental management and health risk control of areas impacted by metal-rich coal combustion.

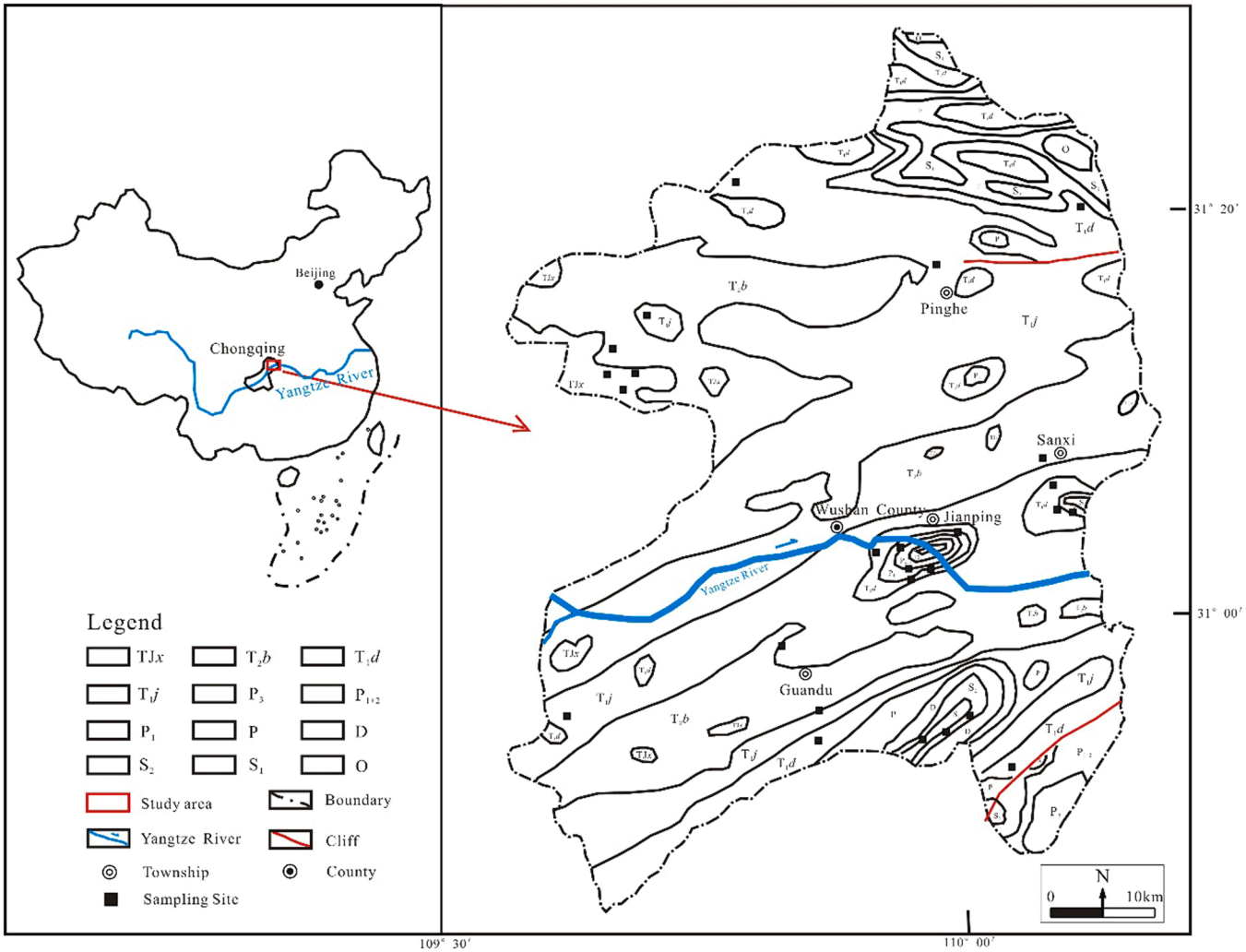

Fig. 1. Sketch map showing the sampling sites of coal-related samples from Wushan County.

2. Materials and methods

2.1. Study area

The study area, Wushan County (109°33′-110°11′ E, 30°45′-31°28′ N) is geographically located in the upper and middle Yangtze River near the headwaters of the Three Gorges Region in eastern Chongqing, SW, China (Fig. 1). Wushan is one of the districts whose karst physiognomy is well developed and concentrative distributed in China, this area is also a traditionally agricultural production base and tourism destination of Chongqing. The main types of soil are purple soil, yellow soil, lime soil, and paddy soil in Wushan County. Cultivated land and woodland are the main utilization patterns of soil in these regions, with average rates of 15.13 % and 64.50 % (Yao et al., 2012).

Wushan has been of concern due to the historic endemic fluorosis induced by local indoor coal combustion. Jianping, a rural area in the south-center of Wushan County has been noted to have one of the most serious historic coal combustion-related fluorosis in China (Liu et al., 2013; Zhou et al., 2009). There are few heavy-polluting industries in the rural area. The local residents used to utilize F-rich coals for cooking and heating, but stopped this practice and began using low-F coals imported from outside areas after 2000. However, sporadic indoor combustion of local inferior coals and past coal mining activities have led to negative impacts on the local environment and human health (Hua et al., 2018).

The rural area of Jianping is composed of a karst landscape and the outcroppings are made up of limestone, dolomite, siltstone, siliceous carbonate rock, claystone, and coal seam from the Permian to the Triassic periods. The local coal strata are composed of a suite of carbonaceous shales interbed with coal seams from the lower Permian Longtan formation, Wujiaping formation, and the lower Triassic Xujiahe formation (Kuang, 1987).

2.2. Sample collection, preparation, and analysis

A total of 33 coal-related samples from 26 sampling sites made up of 17 coals, 5 stone coals, 7 coal gangues, and 4 coal balls for indoor combustion were collected from Wushan County. Among them, 10 coal-related samples were from coal-burning fluorosis areas in the Jianping area while 23 samples were from outside this area. The samples were kept in polyethylene bags to prevent contamination and air-dried. All the samples were crushed and ground to pass a 200 mesh (75 μm) for analysis. To determine element concentration, 50 mg of powdered sample was oxidized with a 4 ml mixture of nitric acid and hydrofluoric acid solution inside a Teflon steel pressure bomb for 24 h at 170 °C. After cooling, 2 ml of 30 % hydrogen peroxide was added to decompose organic matter, then the bomb was heated on a hotplate to remove F. The final solution was made up to 20 ml by the addition of 5 % nitric acid solution (Wang et al., 2004). The liquid tests were determined using an inductively coupled plasma mass spectrometrometer (ICP-MS, Agilent, 7700x, America). To minimize external pollution, guaranteed grade reagents and Milli-Q water (18.2 MΩ·cm) were used throughout all the experiments. International coal-certified reference material (BCR 180), reagent blanks, and duplicates were digested and analyzed in the same condition for analytical quality control. Furthermore, internationally-certified reference materials (SLRS-5) and internal standards (Rh: 500 mg/L) were utilized during the tests. The relative standard deviation (RSD) of replicates was < 10 %, which indicated an acceptable analytical precision. Analytical accuracy expressed as recoveries of the reference material was 95–105 % in this study. Element contents in reagent blanks were always < 2 % of the measured content in the sample. The precision and recovery of these tests were on par with analytical standards.

2.3. Coal combustion trial test

To reveal the retention and transport characteristics of toxic elements in coals during the combustion process, selected Cd-rich coal-related samples that included 4 stone coals (SC1-SC4), 3 coals (C5-C7), and 1 coal ball (CB8) from the study area were used. Each inferior coal powder (weight of 30 g at 200 mesh) was burned in a high-temperature vacuum tube furnace (MTI, GSL-1700X, China) at 1000 °C and held there for 30 min. A mixture of N_2 and O_2 gas (9:1) was used as the combustion atmosphere employing a total gas flow rate of 1 L/min (Yang et al., 2016; Zhou et al., 2012). Under the given condition, all the samples burned completely. A cyclone separator (DEKATI, S110, Finland) and tail gas absorption liquid (0.5 M HNO_3) were installed after the tube furnace throughout the trial to separate combustion ash, slag, and tail gas (Wei et al., 2012). The fly ash collected by the separator had a cut-off size of ~ 2.5 μm. A total of 119 coal combustion byproducts, composed of chars, bottom ashes, fly ashes, and tail gas absorbers were collected and analyzed.

Single factor and orthogonal experiments were applied to determine the influence of combustion atmosphere, temperature, and residence time on the behavior of toxic elements during inferior coal burning (Qi, 2002). Each test consumed 2 g of inferior coal powder for each different condition in the tube furnace. For each single factor experiment, the combustion temperature study was done under the atmosphere of static air by removing the flange during heating at 500, 600, 700, 800, 900, 1000, 1100, and 1200 °C for 30 min, respectively. The combustion atmosphere study was conducted on SC1 with a mixture of N_2 +O_2 during heating at 1000 °C for 30 min. The oxygen gas flow rates in this test were 0, 0.2, 0.4, 0.6, 0.8, 1.0 L/min, respectively. The combustion residence time study conducted on SC1 was done under the atmosphere of static air during heating at 750 °C for 2, 4, 6, 8, 10, 15, 20, 25, and 30 min, respectively. In addition, SC1 was also used to accomplish orthogonal experiments whereby 16 sets of combustion conditions were sieved via an orthogonal method.

2.4. Mineral analysis

To study the mineral compositions of inferior coals during the combustion process, the feed coal, fly ash and bottom slag of SC1 was selected for mineral analysis utilizing X-ray powder diffraction. The mineral composition was examined using X-ray powder diffraction (XRD, Empyrean, Netherlands) with Cu-K_α radiation operating from 4° to 70° 2θ, with a step increment of 0.02° and a counting time of 25 s per step. The minerals in each case were identified by referencing the ICDD powder diffraction file using the JADA 6 software.

3. Results and discussion

3.1. Concentration of harmful elements in coal-related samples

In comparison to other Chinese coals, the coals of Wushan County were featured with elevated contents of trace elements (Table 1). In general, the concentration of trace elements followed the order: stone coals > gangues > coal balls > coals. The average concentration coefficient (CC) of trace elements in the local coals was normalized by the previously reported concentrations of Chinese coal (Dai et al., 2012) to evaluate the enrichment degree of elements in our coal (Fig. 2).

According to Fig. 2, the overall results showed that the local coals presented slightly enriched contents of harmful elements, but the stone coals and gangues enriched in higher concentrations. Cd was the most notable trace metal that was unusually enriched in the stone coals (CC = 137.19 ± 222.99) and significantly enriched in the gangues (CC=53.29 ± 127.25). In contrast, the CC values of Ga, As, and Ta in all the coal-related samples ranged from 2 to 5, suggesting a slight enrichment in the local coal samples. However, the CC values of the coal-related samples for V, Cr, Se, and Mo fluctuated with sample species, and followed the sequence: stone coals > gangues > coals > coal balls. More specifically, these four elements were significantly higher in the stone coals with an average CC of 11.54–28.37, while in the coal

Table 1
Concentration of elements of interest in coal-related samples from Wushan County.

Samples	Location	Cr mg/kg	As mg/kg	Cu mg/kg	Zn mg/kg	Mo mg/kg	Cd mg/kg	Sb mg/kg	Tl mg/kg	S %	Ca %	Fe %
Concentration of typical inferior coal-related samples used for the combustion experiments												
SC1	Jianping	1050	21.7	123.5	1275.2	341.0	146.5	7.39	3.44	2.37	4.71	2.21
SC2	Jianping	55	3.4	156.2	479.1	14.1	22.1	1.98	0.22	0.42	1.09	1.45
SC3	Jianping	1135	9.3	120.5	132.3	11.8	23.6	5.38	1.22	0.22	0.50	1.07
SC4	Jianping	242	7.0	141.7	143.4	25.4	7.2	2.79	0.35	1.71	5.94	3.72
C5	Sanxi	102	46.1	90.5	328.2	20.5	3.1	4.89	1.50	1.29	5.98	2.35
C6	Pinghe	61	22.9	200.3	104.6	11.7	2.5	1.41	0.30	0.17	0.37	2.76
C7	Guandu	21	3.6	47.4	101.5	12.2	3.7	0.58	0.08	0.34	1.14	2.76
CB8	Jianping	97	8.6	138.0	98.2	17.9	6.0	2.00	0.34	0.62	1.05	2.85
Concentration of coal-related samples from Wushan County												
Coals		38.9 ± 20.6	6.29 ± 7.15	62.9 ± 49.7	55.0 ± 73.9	6.66 ± 4.57	1.18 ± 0.84	1.28 ± 1.77	0.21 ± 0.06	–	–	–
Coal Balls		50.8 ± 31.9	11.23 ± 8.16	85.7 ± 53.5	79.0 ± 23.3	8.35 ± 7.11	1.83 ± 2.80	2.17 ± 1.63	0.43 ± 0.16	–	–	–
Stone Coals		504.8 ± 543.1	9.06 ± 7.46	115.0 ± 47.7	454.4 ± 479.5	80.06 ± 146.01	39.95 ± 60.37	3.58 ± 2.80	1.08 ± 1.39	–	–	–
Gangues		179.1 ± 214.1	9.53 ± 7.58	64.3 ± 70.6	124.9 ± 145.6	36.58 ± 61.86	13.32 ± 31.81	3.51 ± 4.89	0.96 ± 1.19	–	–	–
Chinese Coals[a,b]		15.4	3.79	17.5	41.4	3.08	0.25	0.84	0.47	1.14	0.88	3.40
World Coals[c]		16	8.3	16	23	2.2	0.22	0.92	0.63	–	–	–

Jianping, Sanxi, Pinghe, and Guandu are the townships of Wushan County.
SC- stone coal, CB-coal ball, C - coal.
[a] Dai et al. (2012).
[b] Tang et al. (2015).
[c] Ketris and Yudovich (2009).

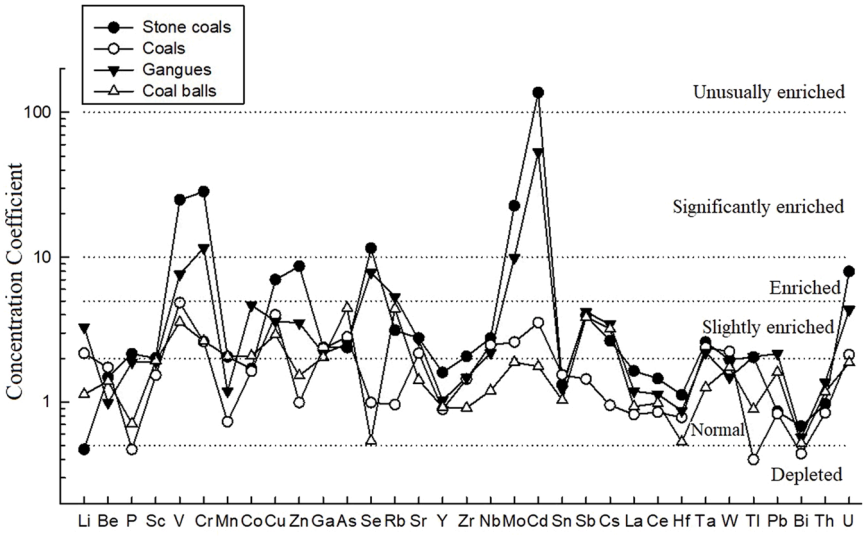

Fig. 2. Scatter plot of average concentration coefficients (CC= ratio of element concentration in coals in selected area vs. average concentrations in Chinese coals) of elements in coal-related samples from Wushan County.

balls and coal samples they were found to be normal to slightly enriched. On the other hand, CCs of V, Se, and Mo were found to be enriched in the gangues with mean CC values of 7.61, 7.86, and 9.93, respectively. Elements like Cu, Zn, and U were found to be enriched in stone coals with average CCs of 7.00, 8.68, and 7.98, respectively. Trace elements of Be, P, Sc, Mn, Co, Y, Zr, Sn, La, Ce, Hf, W, Pb, Bi, and Th were found to be in a normal range with all the coal-related samples having CCs of 0.5–2. Meanwhile, CCs of elements like Rb, Sb, Cs, Ta, and Tl in coals were found to be much lower in comparison to other coal-related samples from Wushan County.

The variations in the elements found in the stone coals, coal, gangue, and coal balls may arise from the way in which the parent coal material was formed, its sedimentary environment as well as hydrothermal fluid variation and epigenesis (Arbuzov et al., 2011; Chen et al., 2011). Previous studies have also indicated that coal seams from the Permian and Triassic periods are characterized by a higher content of the trace elements as observed herein (Querol et al., 2001; Ren et al., 1999; Shen et al., 2013).

Eight inferior coal-related samples from the study area were selected for combustion trial tests, and the concentrations of trace metals are listed in Table 1. Compared to the Chinese and world coals, the typical inferior coal samples were characterized by significantly higher contents of Cd, Mo, Cr, Cu, Zn, As, and Sb. For example, the average concentration of those elements in our stone coals was 199.4, 31.8, 40.3, 7.7, 12.3, 2.7, and 5.2 times greater than Chinese coals. While the data in our coals were found to be 12.4, 4.8, 4.0, 6.4, 4.3, 6.4, and 2.7 times higher with respect to Chinese coals. Meanwhile, the concentration of the aforementioned elements found in our typical coal ball samples were 24.0, 5.8, 6.3, 7.9, 2.4, 2.3, and 2.4 times higher relative to the Chinese coal, respectively. Hence, we can assume based on this data that long-term use of inferior coal for combustion indoors without proper ventilation in under-developed remote rural areas of Wushan County might result in

excessive exposure of toxic elements to the environment and human health.

3.2. Emission of toxic elements during coal combustion

A total of 8 groups of coal-related samples were burned at different temperatures to determine the influence of the release behavior on the harmful elements during the inferior coal-burning process. The influence of combustion parameters such as atmosphere, temperature, and residence time on the release of elevated elements during inferior coal burning was analyzed through orthogonal experiments and range analysis. A typical inferior coal sample (SC1) was used to accomplish our orthogonal experiments. The orthogonal factors are listed in Table 2, whereby 16 sets of combustion experimental conditions were sieved via an orthogonal method. Exhalation rates of some elevated elements for the slags of SC1 were also calculated in this study (Table 3).

According to the range analysis, the combustion temperature was the most important factor for Cd emission in SC1. The ranges of Cd exhalation rates exhibited the following trend: combustion temperature (44.41 %) > combustion atmosphere (16.98 %) > combustion resident time (8.71 %). In addition, the emission characteristic of Tl was similar to Cd, giving ranges of 21.6 %, 4.14 %, and 2.96 % for temperature, atmosphere, and time. Range analysis of the releasing rates for Zn in SC1 followed the order: combustion temperature (16.28 %) > combustion resident time (8.94 %) > combustion atmosphere (8.77 %). Other elevated elements, such as Mo, Cr, Cu, Sb, and As followed a similar trend to Zn. Based on the above results, we can infer that the combustion temperature played a major role in the emissions from elevated elements of inferior coal during our combustion experiments. Liu et al. (2010) also found similar behavior for Cd and Zn release during coal combustion and that the combustion temperature was the primary factor for metal vaporization.

The change of elements upon a single factor combustion temperature varied greatly with the type of element and sample as demonstrated in Fig. 3. The concentration of Cd in slags of most coal-related samples (except for SC4) changed slightly in the temperature range of 500–900 °C, and then maintained a decreasing tendency when the temperature reached 1000–1200 °C. More specifically, Cd in slags of SC1 usually remained at a stable content range (~100 mg/kg), and the exhalation rate was about 45 % during 500–900 °C (Fig. 3). After which, the concentration of Cd in the slags mostly began to decrease with increasing temperature and the decreasing rate was generally greater in comparison to other stone coal samples. Hence, this phenomenon indicated that the combustion temperature played an important role in the Cd emission to the environment. Moreover, the Cd contained in the inferior coal showed significant vaporization when the combustion temperature increased.

Likewise, Sb, Zn, and Tl showed similar trends with Cd in the slags of stone coals. Since it is known that the volatility of toxic elements depends on the occurrence mode(s) as well as the mineral carriers (Izquierdo and Querol, 2012), and elements interacting with the mineral, the stability observed above for all the coal-related samples may in part be due to some of these factors (Yu et al., 2011). Stone coal samples from our research area contained carbonate and monosulfide fractions (Xiong et al., 2017) and it was found that Ca, Fe, and S in those inferior coal-related samples were 2.60 ± 2.49 %, 2.40 ± 0.84 %, and 0.89 ± 0.81 % (Table 1), respectively. The presence of these carbonate and monosulfide fractions makes it easier for toxic elements to be released into the environment. It is well known that a higher combustion temperature promotes the rate of coal decomposition (Yu et al., 2011), and as such destroys these fractions (Parshetti et al., 2013) causing the release of elements. This is in agreement with previous works (Mecozzi and Scaccia, 2012; Wang et al., 2015), and further highlights the importance of temperature on the behavior of the toxic elements.

The concentration of Cu and Cr increased between 500 and 600 °C in SC1–3 slags but then changed little as the temperature increased. In contrast, Cu and Cr remained at a stable value in SC4, C5, and C6 throughout the whole experiment. In the case of CB8, these two elements showed a slight increase when the temperature was 1100–1200 °C. Interestingly, a double peak phenomenon occurred for As between 500 °C and 900 °C for the SC4 and C6 samples with an overall decreasing trend for the latter (Fig. 3). This observed trend is similar to previous studies done on Guizhou coals where the concentrations of As in coal ash varied with different particle sizes and temperatures but the bimodal mode was also displayed during combustion (Zhao et al., 2008).

Mo in slags formed from various temperatures are characterized with having a high concentration (> 10 mg/kg) and as such, combustion of these slags may release it into the environment. Except for SC2, the content of Mo in the slags largely remained constant during 500–800 °C. The only samples that showed clear variations in Mo concentration at temperatures > 800 °C were C6 (slight decrease) – C7 (increase). It is known that calcium can have a significant influence on the release of elements during coal combustion (Zhao et al., 2008) and the alkalinity of the slags may accelerate the release of Mo (Izquierdo and Querol, 2012). As such, some of the various trends observed for the coal samples may be due to the calcium content in our slags. Calcium additives might be a viable option for improving the adsorption ability of slag on elements during the combustion process of Cd-rich coal.

SC1 was selected for single factor and orthogonal experiments. The results from the single factor study on the combustion residence time (Fig. 4a) indicated that concentrations of Cr, Zn, Mo, Cu, Cd, and Sb were fairly constant as the combustion time progressed. In contrast, As and Tl displayed minimum values between 15 and 20 min. Based on this variation tendency, we may conclude that residence time plays a less important role for releasing toxic elements in comparison to temperature. This result is the same as what was observed during the orthogonal experiments.

The concentration variation trend for the elevated trace element as a function of oxygen rate is shown in Fig. 4b. In general, the concentrations of Cr, Zn, Mo, Cu, and As largely remained constant with increasing oxygen content. Meanwhile, a minimum concentration of Cd occurred in SC1 when the combustion oxygen rate was 0.2 L/min, which then increased with oxygen content until it reached its highest concentration at 1.0 L/min. This tendency was similar to Sb and Tl but the change occurred instead at O_2 = 0.4 L/min (Fig. 4b).

This indicated that the Cd, Sb, and Tl in SC1 were readily emitted under a low oxygen environment. Hence, increasing the oxygen rate may lower the vaporization of some toxic elements like Cd, Sb, and Tl. This trend observed above may indicate that reducing environments promote higher emission of these elements and our study is consistent with previous findings (Guo et al., 2004; Yi et al., 2015; Yu et al., 2011). Hence, these results suggest that oxygen is an important factor in the emission of some elevated elements from inferior coal. As such, these types of inferior coal should be combusted under well-oxygenated conditions to avoid large quantities of toxic element outflows to the environment.

Table 2
Orthogonal factors used during inferior coal (SC1) combustion.

Factor Level	A	B	C	
	Temperature (℃)	Time (min)	O_2 (L/min)	N_2 (L/min)
1	500	5	0.2	0.8
2	700	10	0.4	0.6
3	900	15	0.8	0.2
4	1100	20	1.0	0.0

Each factor contained 4 levels, and all of the condition factors are randomly arranged in the orthogonal experiment.

Table 3
Exhalation rates and range analysis of orthogonal experiments during inferior coal (SC1) combustion.

Experimental conditions			Exhalation rate (%)							
Temperature	Time	O_2	Cr	As	Cu	Zn	Mo	Cd	Sb	Tl
1	1	1	6.02	96.23	31.34	57.08	16.97	73.75	26.04	72.27
1	2	2	2.46	96.47	27.07	57.68	13.55	95.68	33.42	71.22
1	3	3	4.94	96.63	29.63	66.50	16.27	94.27	39.92	79.51
1	4	4	2.33	96.69	25.16	85.45	14.76	98.53	44.63	83.77
2	1	2	3.12	96.33	27.45	51.05	14.27	47.13	23.76	63.80
2	2	1	2.74	96.14	26.05	48.66	14.25	37.66	21.17	63.63
2	3	4	2.35	96.43	26.75	51.02	12.57	72.24	22.72	62.27
2	4	3	3.10	96.29	27.31	50.85	12.10	45.12	21.52	61.20
3	1	3	5.66	96.47	26.39	52.14	14.83	45.07	26.41	59.13
3	2	4	5.29	96.46	28.56	53.40	14.81	46.76	25.21	58.63
3	3	1	3.09	96.28	28.20	52.82	15.72	42.18	25.76	57.65
3	4	2	18.68	96.75	39.22	58.91	27.94	50.60	35.64	62.44
4	1	4	6.45	96.00	32.98	57.31	16.40	51.10	29.07	59.10
4	2	3	1.96	96.15	28.23	53.25	14.17	47.14	25.43	55.76
4	3	2	0.99	96.09	23.46	48.37	11.39	43.20	23.15	51.86
4	4	1	2.85	96.25	27.65	53.54	13.83	47.14	27.02	53.67
Range analysis	Temperature	K1/4	3.94	96.51	28.30	66.68	15.39	90.56	36.00	76.69
		K2/4	2.83	96.30	26.89	50.40	13.30	50.54	22.29	62.73
		K3/4	8.18	96.49	30.59	54.32	18.33	46.15	28.26	59.46
		K4/4	3.06	96.12	28.08	53.12	13.95	47.15	26.17	55.10
		Range	5.35	0.38	3.70	16.28	5.03	44.41	13.71	21.60
	Time	K1/4	5.31	96.26	29.54	54.40	15.62	54.26	26.32	63.58
		K2/4	3.11	96.31	27.48	53.25	14.20	56.81	26.31	62.31
		K3/4	2.84	96.36	27.01	54.68	13.99	62.97	27.89	62.82
		K4/4	6.74	96.50	29.84	62.19	17.16	60.35	32.20	65.27
		Range	3.90	0.24	2.83	8.94	3.17	8.71	5.90	2.96
	O_2	K1/4	3.68	96.23	28.31	53.03	15.19	50.18	25.00	61.81
		K2/4	6.31	96.41	29.30	54.00	16.79	59.15	28.99	62.33
		K3/4	3.92	96.39	27.89	55.69	14.34	57.90	28.32	63.90
		K4/4	4.11	96.40	28.36	61.80	14.64	67.16	30.41	65.94
		Range	2.64	0.19	1.41	8.77	2.45	16.98	5.41	4.14

K1: summation of exhalation rates of an element in factor level 1.
K2: summation of exhalation rates of an element in factor level 2.
K3: summation of exhalation rates of an element in factor level 3.
K4: summation of exhalation rates of an element in factor level 4.

3.3. Distribution of toxic elements in byproducts of coal combustion

Harmful element concentrations in typical coal-related samples and combustion byproducts from our research area are listed in Table 4. Out of all the combustion products (bottom slag, fly ash, and tail gas absorber) from the stone coal, coal, and coal ball, the concentration of elevated elements in the fly ash was the highest. In particular, elements like As, Mo, Sb, Cr, Cu, and Zn were in higher concentration after coal combustion in the fly ash. This is in agreement with observations from low-sulfur bituminous coals of America, where the greatest median concentrations of toxic elements were found in the fine-grained fly ash products (Yang et al., 2019; Swanson et al., 2013).

The enrichment ratio (ER), partition ratio (PR), and enrichment factor (EF) with respect to Fe were calculated for elevated elements in this study per Eqs. (1–3).

$$ER = C_{\text{element in fly ash (or bottom slag)}} / C_{\text{element in feed coal}} \quad (1)$$

$$PR = C_{\text{element in fly ash}} / C_{\text{element in bottom slag}} \quad (2)$$

$$EF = (C_{\text{element}}/C_{\text{Fe}})_{\text{fly ash}} / (C_{\text{element}}/C_{\text{Fe}})_{\text{feed coal}} \quad (3)$$

The ER value is defined as the ratio of element content in ash (or slag) to the concentration of that element in feed coal. Usually, ER values higher than 1.6 indicate the enriched state of an element in the ash (or slag), while a value of less than 0.6 represented a depleted state (Bellagamba et al., 1993). The PR value is the content ratio of an element in the fly ash relative to the element in the bottom slag. Based on the partition and enrichment behavior of an element, Xu et al. (2003) classified three basic groups of trace elements.

Average ER values of As were 19.61, 30.18, and 23.32 in fly ash of typical stone coals, coals, and coal balls (Fig. 5a). In contrast, average As ER values in the bottom slags of those samples were only 0.39, 1.02, and 0.68 (Fig. 5b). In particular, high PR values of 36.35 ± 13.45 for As were determined in typical coal-related samples (Fig. 5c). Hence based on these results, As was found to be significantly enriched in the fly ash. In addition, the average PR values of Mo, Sb, Cr, Cu, and Zn were 3.12, 1.55, 1.38, 1.19, and 1.63, respectively. The average ER values of fly ash for these aforementioned elements were 1.88–4.60, while ERs of these elements in the bottom slags were equal to1.6 or less than 0.6. In this study, it was observed that elevated elements in typical coal-related samples belong to group II, and these were enriched in fly ash after combustion (Xu et al., 2003). Thus exerting a negative effect on the environment.

The EF values were calculated for elements in the bottom slags and the fly ash to understand the distribution pattern of these elevated elements in the coal combustion byproducts. The results indicated that As, Mo, Sb, Cr, and Zn were enriched in the fly ash of our inferior coal-related samples from the study area giving average EF values of 12.25, 2.14, 1.41, 1.98, and 1.53, respectively. In particular, the mean EF values of fly ash from the coals followed the order: As (13.92)›Cr (2.78)›Zn (1.69)›Sb (1.29)›Mo (1.02)›Tl (0.76)›Cd (0.52). Meanwhile, the average EF values of stone coal ash followed a descending order: As (11.51)›Mo (2.90)›Sb (1.48)›Zn (1.47)›Cr (1.36)›Tl (0.69)›Cd (0.68). Coal ball ash samples displayed EF values for As, Mo, Cr, Sb, Zn, and Tl that were 10.20, 2.48, 2.04, 1.50, 1.25, and 1.17, respectively.

Thus, as we can see from these trace elements results of coal combustion byproducts, they tended to accumulate in fly ash with As showing the highest volatility among other elements. This is in agreement with previous works (Hower et al., 2020; Srikanth and Naga Raju, 2019). Once burned, As and other toxic elements may react with the calcium in the coal samples producing X-Ca (where X is As and other

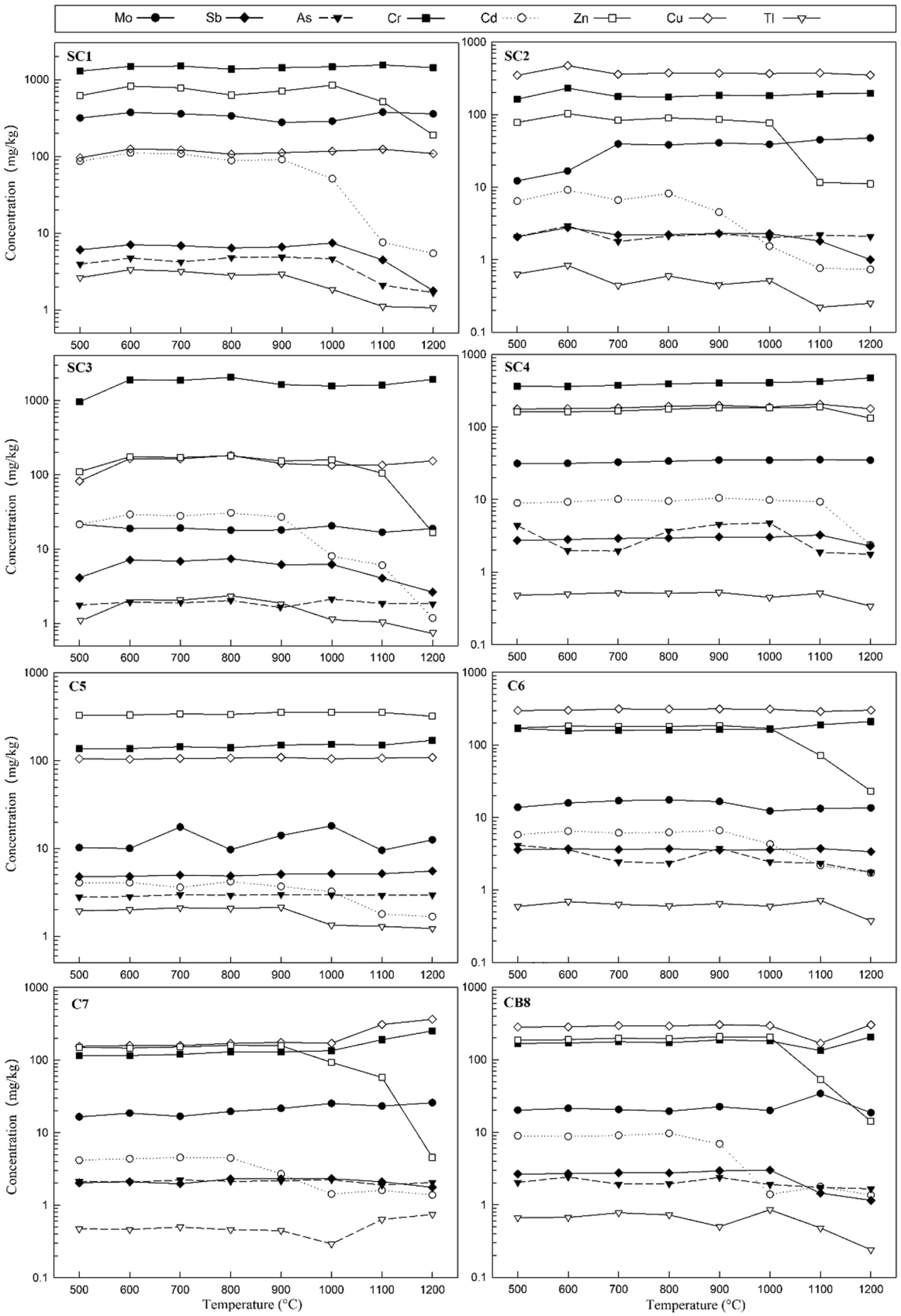

Fig. 3. Scatter plots showing the concentration of elevated elements as a function of temperature from our coal combustion slags. Each powder (2 g) was burned in a tube furnace under the atmosphere of air for 30 min.

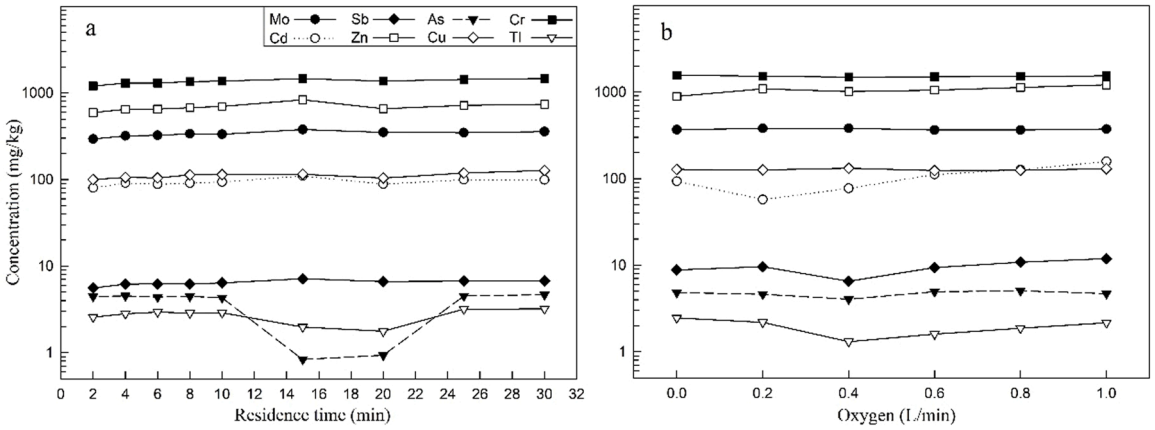

Fig. 4. Scatter plots of elevated elements in slags of stone coal (SC1) from a single factor coal combustion experiment. (a) represents the scatter diagram of elements in slags that were burned at different residence times. This experiment conducted on SC1 was done under the atmosphere of static air during heating at 750 °C for 2, 4, 6, 8, 10, 15, 20, 25, and 30 min, respectively. (b) shows the scatter diagram of elements in slags that were burned with different rates of oxygen. This experiment was conducted on SC1 at 1000 °C for 30 min using oxygen gas flow rates of 0, 0.2, 0.4, 0.6, 0.8, and 1.0 L/min, respectively.

Table 4
The concentration of toxic elements from typical inferior coals and combustion products (bottom slag, fly ash, and tail gas absorber) from Wushan County.

Sample	Type	Cd	As	Mo	Sb	Cr	Cu	Zn	Tl
SC1	Feed coal	83.6	4.5	289.0	5.5	1160	99	610	2.6
	Bottom slag	67.8	2.4	385.0	7.4	1500	132	833	1.5
	Fly ash	101.0	97.7	434.0	12.0	2060	166	1010	1.7
	Tail gas absorber	1.08	0.01	1. 78	0.02	1.80	2.48	5.50	0.11
SC2	Feed coal	3.2	4.3	15.1	0.9	71	149	36	0.3
	Bottom slag	1.0	2.3	43.2	2.3	197	382	76	0.4
	Fly ash	3.2	127.0	74.1	4.4	364	374	185	0.6
	Tail gas absorber	1.00	0.01	1.00	0.02	0.39	0.93	2.25	0.02
SC3	Feed coal	20.2	4.7	17.1	4.7	1245	109	120	1.4
	Bottom slag	15.5	2.2	20.8	6.7	1705	147	168	1.2
	Fly ash	16.4	56.0	173.0	8.6	1820	223	279	1.6
	Tail gas absorber	0.20	0.01	0.87	0.01	1.21	0.56	1.59	0.01
SC4	Feed coal	7.9	4.2	27.1	2.4	307	149	143	0.4
	Bottom slag	8.5	2.1	38.7	3.0	427	196	185	0.4
	Fly ash	9.8	64.2	51.2	4.1	518	194	222	0.4
	Tail gas absorber	1.70	0.05	1.49	0.03	17.72	5.45	192.89	0.10
C5	Feed coal	3.3	1.8	6.6	3.8	109	84	261	1.6
	Bottom slag	3.8	2.5	28.1	5.3	158	111	361	1.8
	Fly ash	2.2	49.0	5.9	2.3	155	91	239	0.9
	Tail gas absorber	2.03	0.04	1.29	0.04	17.25	5.75	214.59	0.12
C6	Feed coal	3.4	2.4	7.5	0.7	73	153	91	0.4
	Bottom slag	1.4	2.3	23.8	1.2	144	285	171	0.5
	Fly ash	3.8	70.9	0.8	6.8	299	305	332	0.8
	Tail gas absorber	0.40	0.01	1.23	0.01	0.70	0.78	1.72	0.02
C7	Feed coal	1.4	3.7	5.7	0.5	25	355	33	0.1
	Bottom slag	0.8	2.4	63.4	2.2	140	174	121	0.3
	Fly ash	3.5	125.0	54.3	7.0	632	401	403	0.4
	Tail gas absorber	0.20	0.00	0.69	0.01	0.27	0.84	1.70	0.01
CB8	Feed coal	4.9	3.7	7.6	1.4	87	149	98	0.3
	Bottom slag	0.9	2.5	38.9	2.5	199	327	171	0.4
	Fly ash	3.9	86.3	43.1	4.8	405	295	281	0.8
	Tail gas absorber	0.40	0.02	1.08	0.01	0.38	0.67	3.41	0.01

Each sample (30 g) was burned with a mixture atmosphere (N_2 = 0.9 L/min, O_2 = 0.1 L/min) at 1000 °C for 30 min.
The unit for the feed coal, bottom slag, and fly ash is in mg/kg.
The unit for the tail gas absorber is in μg/L.

elements) super-micron particles (Seames and Wendt, 2000) and as such one method to reduce the volatilization of trace elements of inferior coal byproducts maybe through the addition of 20–30 % biomass or calcium oxide (Zhao et al., 2008; Zhou et al., 2015).

In contrast, the EFs of Cd, As, Sb, Cu, Zn, and Tl in the bottom slags were usually < 1 (not significant contributors), while the average data for Mo and Cr was 1.64 and 1.02, respectively. Among the 3 types of coal samples, the coal ball contributed the highest EF for Mo with a value of 2.48. Thus indicating that Mo was moderately enriched in coal balls after combustion, and that clay minerals might be the leading cause of enrichment (Xu et al., 2013).

Cells exposed to high concentrations of coal and coal fly ash particles with significant contents of toxic elements might induce cytotoxic effects and chromosomal instability (Leon-Mejia et al., 2016). Numerous studies have shown that the particle size of chars plays an important effect on the distribution pattern of toxic elements after coal combustion (Hower et al., 2020; Juda-Rezler and Kowalczyk, 2013; Yu et al., 2011). Since the concentration of trace elements increased with the decreasing particle size of the fly ash (Lanzerstorfer, 2018), fine particles formed by coal fire not only can exhibit a high migration capacity but also tends to

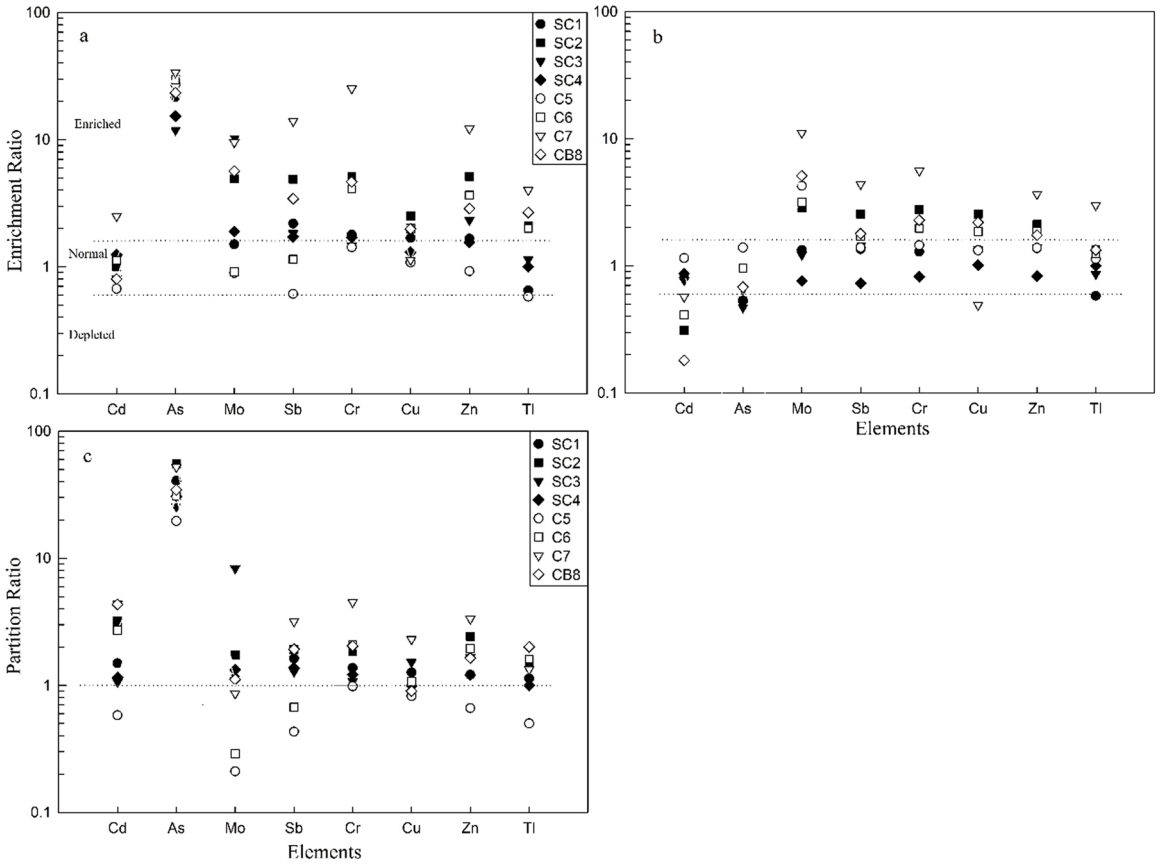

Fig. 5. Scatter plots displaying the enrichment ratio (ER) and partition ratio (PR) of elevated elements from typical Cd-rich inferior coals. Each sample was burned with a mixture atmosphere (N_2 =0.9 L/min, O_2 =0.1 L/min) at 1000 °C for 30 min. (a) represents the scatter diagram of ERs in fly ash, (b) represents the scatter diagram of ERs in bottom slags, (c) shows the scatter diagram of PRs in coal combustion products.

contain high contents of toxic elements. This in turn may cause serious damage to the environment and human health. In contrast, coarse particles such as those from bottom slag that often contain less concentration of toxic elements and in turn may have a lower impact on the environment and human health (Diao et al., 2021; Hilker et al., 2021; Swanson et al., 2013; Wang et al., 2009; Yi et al., 2008).

3.4. Mineralogical characterization

Previous studies have noted that the mineral composition of the feed inferior coal (SC1) was dominated by quartz, kaolinite, calcite, dolomite, muscovite, and albite (Xiong et al., 2017). The mineral associations of coal combustion byproducts were varied by considering a different combustion atmosphere and coal inhomogeneity.

Mineralogical characterization of the SC1 combustion products was remarkably affected by the type of combustion atmosphere. The XRD results indicated that SC1 samples burned without oxygen contained the largest number of phases (lizardite, calcite, dolomite, forsterite, and enstatite) (Fig. 6a). This is because the crystal structure and oxygen atom in lattices of clay minerals changed during anoxic combustion (Gong et al., 2020). Upon the addition of 0.2 L/min O_2 during combustion (Fig. 6b), the majority of the previous silicates decomposed leaving only calcite. Further addition of 0.4 g/L O_2 resulted in the formation of quartz and anhydrite (Fig. 6c). The combustion slag formed after burning using 0.6 L/min of O_2 contained dolomite, calcite, and actinolite (Fig. 6d). In contrast, those precipitated with 0.8–1.0 L/min of O_2 were dominated by quartz (Fig. 6e-f). It is worth noting that the mineral composition of the bottom slag from SC1 was similar to the slags under well-oxygenated combustion conditions (O_2 = 0.8 L/min and 1.0 L/min) (Fig. 6g). Furthermore, XRD results indicated that the fly ash of SC1 was largely composed of quartz and nacrite (Fig. 6h). The formation of these phases noted above are likely because quartz is the product of partial melting and glass formation from the initial clay minerals (Jak et al., 1998; Zhou et al., 2012) while calcium minerals (e.g. calcite and dolomite) may have reacted with sulfur dioxide to create anhydrite. All in all, the mineral phases presented under these conditions are similar to those reported from lignite ash (Singh et al., 2011).

4. Conclusions

This study illustrated the emission characteristic, distribution patterns, and mineral composition of elevated elements in combustion products of Cd-rich coals from Jianping, Wushan County in SW, China. Our results showed that elements like Cd, V, Cr, Se, and Mo in the study area were significantly enriched to unusually enriched in the stone coals (with average CCs of 11.54–137.19), while Cd, V, Se, and Mo were found to be enriched to significantly enriched in the gangues (with mean CC values of 7.61–53.29).

Single factor and orthogonal experiments of coal combustion tests revealed that the combustion condition played an important role in the emission and transformation of elements during the burning of typical inferior coals. The combustion temperature was the primary cause for releasing elevated elements among all of the operational variables studied. More specifically, a high temperature (~1000 °C) promoted the rate of coal decomposition and accelerated the release of Cd, Sb, Zn, and Tl into the environment. At the same time, the combustion residence time may exert a greater influence on the release of As and Tl from inferior coals. Meanwhile, Cd, Sb, and Tl in SC1 were found to be readily emitted under low oxygen environments. To sum up, lower combustion temperature and sufficient oxygen condition might be the practicable

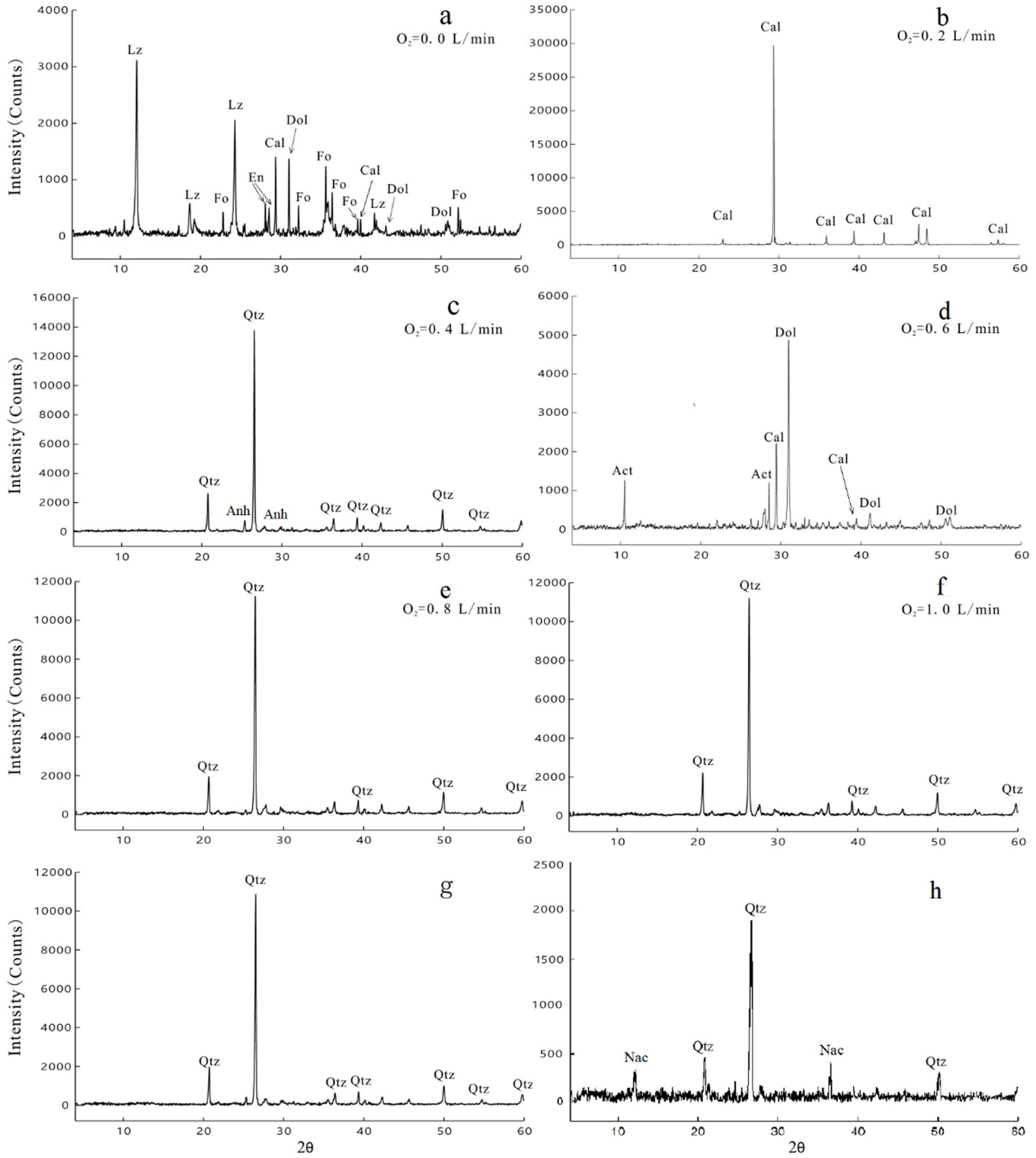

Fig. 6. Powder X-ray diffraction patterns of the combustion products from SC1. (a)-(f) demonstrate the bottom slags after being burned under different combustion atmospheres (O_2 and N_2). Meanwhile, (g)-(h) are for bottom slag and fly ash of SC1 using a reaction temperature of 1000 °C and a residence time of 30 min. The following abbreviations were used for the mineral phases detected: Act, actinolite. Anh, anhydrite. Cal, calcite. Dol, dolomite. En, enstatite. Fo, forsterite. Lz, lizardite. Nac, nacrite. Qtz, quartz.

measures to decrease the emission of harmful elements from Cd-rich coal combustion in the study area.

The coal combustion process caused a large amount of elements to be released from the inferior coal in this study. The elevated elements (As, Mo, Sb, Cr, and Cu) in typical coals tended to accumulate in the fly ash with fine particle sizes. The mineralogical composition changed greatly after coal combustion was done under different oxygen conditions. Anoxia favored silicates and well-oxygenated environments promoted quartz and carbonates.

Declaration of Competing Interest

The authors declare that they have no known competing financial interests or personal relationships that could have appeared to influence the work reported in this paper.

Data availability

Data will be made available on request.

Acknowledgments

This research was supported by the following funding agencies: National Natural Science Foundation of China (41830753), Science and Technology Foundation of Guizhou Province ([2020]1Y165), Guizhou Education Department Youth Science and Technology Talents Growth Project (KY[2019]099), Joint S&T Funds of Science and Technology Department of Guizhou Province and Guiyang University (GYU-KJT [2019]−22), and Youth Innovation Promotion Association CAS (2021399). Dr. Yongchun Zhao from State Key Laboratory of Coal Combustion, Huazhong University of Science and Technology is appreciated for supporting the technical assistances in coal combustion experiments.

References

Arbuzov, S.I., Volostnov, A.V., Rikhvanov, L.P., Mezhibor, A.M., Ilenok, S.S., 2011. Geochemistry of radioactive elements (U, Th) in coal and peat of northern Asia (Siberia, Russian Far East, Kazakhstan, and Mongolia). Int. J. Coal Geol. 86, 318–328.

Bellagamba, B., Caridi, A., Cereda, E., Marcazzan, G.M.B., Valkovic, V., 1993. PIXE application to the study of trace element behavior in coal combustion cycle. Nucl. Instrum. Methods Phys. Res. 75 (1–4), 222–229.

Bernard, R.C., William, A.E., 1984. The Science and Technology of Coal and Coal Utilization. Springer,, Boston, pp. 1–5.

Bhangare, R.C., Ajmal, P.Y., Sahu, S.K., Pandit, G.G., Puranik, V.D., 2011. Distribution of trace elements in coal and combustion residues from five thermal power plants in India. Int. J. Coal Geol. 86 (4), 349–356.

Chen, J., Liu, G.J., Jiang, M.M., Chou, C.L., Li, H., Wu, B., Zheng, L.G., Jiang, D.D., 2011. Geochemistry of environmentally sensitive trace elements in Permian coals from the Huainan coalfield, Anhui, China. Int. J. Coal Geol. 88, 41–54.

Chen, J., Liu, G.J., Kang, Y., Wu, B., Sun, R.Y., Zhou, C.C., Wu, D., 2013. Atmospheric emissions of F, As, Se, Hg, and Sb from coal-fired power and heat generation in China. Chemosphere 90 (6), 1925–1932.

Dai, S., Ren, D., Chou, C.L., Finkelman, R.B., Seredin, V.V., Zhou, Y., 2012. Geochemistry of trace elements in Chinese coals: a review of abundances, genetic types, impacts on human health, and industrial utilization. Int. J. Coal Geol. 94, 3–21.

Dai, W.T., Dong, J.H., Yan, W.L., Xu, J.R., 2017. Study on each phase characteristics of the whole coal life cycle and their ecological risk assessment – a case of coal in China. Environ. Sci. Pollut. Res. 24 (2), 1296–1305.

Deng, S., Shi, Y.J., Liu, Y., Zhang, C., Wang, X.F., Cao, Q., Li, S.G., Zhang, F., 2014. Emission characteristics of Cd, Pb and Mn from coal combustion: field study at coal-fired power plants in China. Fuel Process. Technol. 126 (1), 469–475.

Department of Energy Statistics of National Bureau of Statistics of China, 2021. China Energy Statistical Yearbook of 2020. China Statistical Press, Beijing.

Diao, L.L., Zhang, H.T., Liu, B.S., Dai, C.L., Zhang, Y.F., Dai, Q.L., Feng, Y.C., 2021. Health risks of inhaled selected toxic elements during the haze episodes in Shijiazhuang, China: insight into critical risk sources. Environ. Pollut. 276, 116664.

Dziok, T., Grzywacz, P., Bochenek, P., 2019. Assessment of mercury emissions into the atmosphere from the combustion of hard coal in a home heating boiler. Environ. Sci. Pollut. Res. 26 (22), 22254–22263.

Gong, B.G., Tian, C., Xiong, Z., Yang, Y., Wu, J., Li, W.J., Du, Y., Liu, H., Wang, Y., Zhao, Y.C., Zhang, J.Y., 2020. Effects of temperature, atmosphere, silicon occurrences on fine particle formation from vaporization during high-silicon coal combustion. Fuel 280, 118649.

Guo, R., Yang, J., Liu, Z., 2004. Behavior of trace elements during pyrolysis of coal in a simulated drop-tube reactor. Fuel 83 (6), 639–643.

Haykiri-Acma, H., Yaman, S., Ozbek, N., Kucukbayrak, S., 2011. Mobilization of some trace elements from ashes of Turkish lignites in rain water. Fuel 90 (11), 3447–3455.

Hilker, N., Jeong, C.H., Wang, J.M., Evans, G.J., 2021. Elucidating long-term trends, seasonal variability, and local impacts from thirteen years of near-road particle size data (2006-2019). Sci. Total Environ. 774, 145028.

Hower, J.C., Fu, B., Dai, S.F., 2020. Geochemical partitioning from pulverized coal to fly ash and bottom ash. Fuel 279, 118542.

Hua, C.Y., Zhou, G.Z., Li, R.Y., 2018. Assessment of heavy metal in coal gangue: distribution, leaching characteristic and potential ecological risk. Environ. Sci. Pollut. Res. 25, 32321–32331.

Izquierdo, M., Querol, X., 2012. Leaching behaviour of elements from coal combustion fly ash: an overview. Int. J. Coal Geol. 94, 54–66.

Jak, E., Degterov, S., Hayes, P.C., Pelton, A.D., 1998. Thermodynamic modelling of the system Al_2O_3-SiO_2-CaO-FeO-Fe_2O_3 to predict the flux requirements for coal ash slags. Fuel 77 (1–2), 77–84.

Juda-Rezler, K., Kowalczyk, D., 2013. Size distribution and trace elements contents of coal fly ash from pulverized boilers. Pol. J. Environ. Stud. 22 (1), 25–40.

Ketris, M.P., Yudovich, Y.E., 2009. Estimations of clarkes for carbonaceous biolithes: World averages for trace element contents in black shales and coals. Int. J. Coal Geol. 78 (2), 135–148.

Kuang, Z.G., 1987. Instruction book of Chongqing geological map (1/200000). No.208 Hydrogeology and Engineering Geology Team of Sichuan. Geology and Mineral Bureau.

Lanzerstorfer, C., 2018. Fly ash from coal combustion: dependence of the concentration of various elements on the particle size. Fuel 228 (15), 263–271.

Leon-Mejia, G., Silva, L.F.O., Civeira, M.S., Oliveira, M.L.S., Machado, M., Villela, I.V., Hartmann, A., Premoli, S., Correa, D.S., Da Silva, J., 2016. Cytotoxicity and genotoxicity induced by coal and coal fly ash particles samples in V79 cells. Environ. Sci. Pollut. Res. 23 (23), 24019–24031.

Liu, J., Falcoz, Q., Gauthier, D., Flamant, G., Zheng, C.Z., 2010. Volatilization behavior of Cd and Zn based on continuous emission measurement of flue gas from laboratory-scale coal combustion. Chemosphere 80 (3), 241–247.

Liu, Y., Xiao, T., Ning, Z., Li, H., Tang, J., Zhou, G., 2013. High cadmium concentration in soil in the three gorges region: geogenic source and potential bioavailability. Appl. Geochem. 37, 149–156.

Ma, W.P., Li, Z., Lv, J.F., Yang, L.H., Liu, S.Q., 2021. Environmental evaluation study of toxic elements (F, Zn, Be, Ni, Ba, U) in the underground coal gasification (UCG) residuals. J. Clean. Prod. 297, 14.

Mecozzi, R., Scaccia, S., 2012. Trace Cd, Co, and Pb elements distribution during Sulcis coal pyrolysis: GFAAS determination with slurry sampling technique. Microchem. J. 100, 48–54.

Ministry of Natural Resources of the People's Republic of China, 2018. China statistical bulletin of land, mineral and marine resources.

Oboirien, B.O., Thulari, V., North, B.C., 2014. Major and trace elements in coal bottom ash at different oxy coal combustion conditions. Appl. Energy 129, 207–216.

Orndorff, Z.W., Daniels, W.L., Zipper, C.E., Eick, M., Beck, M., 2015. A column evaluation of Appalachian coal mine spoils' temporal leaching behavior. Environ. Pollut. 204, 39–47.

Parshetti, G.K., Hoekman, S.K., Balasubramanian, R., 2013. Chemical, structural and combustion characteristics of carbonaceous products obtained by hydrothermal carbonization of palm empty fruit bunches. Bioresour. Technol. 135, 683–689.

Qi, Q.J., 2002. The Mechanism and Experimental Studies on Occurrence Characteristic, Combustion Transfer and Pollution Control Technology of Fluorine in Coal. Zhejiang University, Hangzhou.

Querol, X., Alastuey, A., Zhuang, X.G., Hower, J.C., Lopez-Soler, A., Plana, F., Zeng, R.S., 2001. Petrology, mineralogy and geochemistry of the Permian and Triassic coals in the Leping area, Jiangxi Province, southeast China. Int. J. Coal Geol. 48 (1–2), 23–45.

Quick, W.J., Irons, R., 2002. Trace element partitioning during the firing of washed and untreated power station coals. Fuel 81 (5), 665–672.

Ren, D.Y., Zhao, F.H., Wang, Y.Q., Yang, S.J., 1999. Distributions of minor and trace elements in Chinese coals. Int. J. Coal Geol. 40, 109–118.

Saikia, J., Saikia, P., Boruah, R., Saikia, B.K., 2015. Ambient air quality and emission characteristics in and around a non-recovery type coke oven using high sulphur coal. Sci. Total Environ. 530, 304–313.

Seames, W.S., Wendt, J., 2000. Partitioning of arsenic, selenium, and cadmium during the combustion of Pittsburgh and Illinois #6 coals in a self-sustained combustor. Fuel Process. Technol. 63 (2), 179–196.

Shen, J., Algeo, T.J., Feng, Q.L., Zhou, L., Feng, L.P., Zhang, N., Huang, J.H., 2013. Volcanically induced environmental change at the Permian-Triassic boundary (Xiakou, Hubei Province, South China): Related to West Siberian coal-field methane releases? J. Asian Earth Sci. 75, 95–109.

Singh, S., Ram, L.C., Masto, R.E., Verma, S.K., 2011. A comparative evaluation of minerals and trace elements in the ashes from lignite, coal refuse, and biomass fired power plants. Int. J. Coal Geol. 87 (2), 112–120.

Srikanth, S., Naga Raju, G.J., 2019. Quantitative study of trace elements in coal and coal related ashes using PIXE. J. Geol. Soc. India 94, 533–537.

Swanson, S.M., Engle, M.A., Ruppert, L.F., Affolter, R.H., Jones, K.B., 2013. Partitioning of selected trace elements in coal combustion products from two coal-burning power plants in the United States. Int. J. Coal Geol. 113 (3), 116–126.

Tang, J., Xiao, T., Wang, S., Lei, J., Zhang, M., Gong, Y., He, L., 2009. High cadmium concentrations in areas with endemic fluorosis: a serious hidden toxin? Chemosphere 76 (3), 300–305.

Tang, Y.G., He, X., Cheng, A.G., Li, W.W., Deng, X.J., Wei, Q., Li, L., 2015. Occurrence and sedimentary control of sulfur in coals of China. J. China Coal Soc. 40 (9), 1977–1988.

Tian, H.Z., Cheng, K., Wang, Y., Zhao, D., Lu, L., Jia, W.X., Hao, J.M., 2012. Temporal and spatial variation characteristics of atmospheric emissions of Cd, Cr, and Pb from coal in China. Atmos. Environ. 50, 157–163.

Vejahati, F., Xu, Z.H., Gupta, R., 2010. Trace elements in coal: associations with coal and minerals and their behavior during coal utilization – a review. Fuel 89, 904–911.

Wang, J., Nakazato, T., Sakanishi, K., Yamada, O., Tao, H., Saito, I., 2004. Microwave digestion with HNO_3/H_2O_2 mixture at high temperatures for determination of trace elements in coal by ICP-OES and ICP-MS. Anal. Chim. Acta 514, 115–124.

Wang, W.F., Yong, Q., Wang, J.Y., Jian, L., 2009. Partitioning of hazardous trace elements during coal preparation. Proc. Earth Planet. Sci. 1 (1), 838–844.

Wang, X.B., Xu, Z.X., Wei, B., Zhang, L., Tan, H.Z., Yang, T., Duic, N., 2015. The ash deposition mechanism in boilers burning Zhundong coal with high contents of sodium and calcium: a study from ash evaporating to condensing. Appl. Therm. Eng. 80, 150–159.
Wei, X.F., Zhang, G.P., LI, L., Xiang, M., Cai, Y.B., 2012. Distribution and enrichment of trace elements in coal combustion products from Southwestern Guizhou. Environ. Sci. 33 (5), 1457–1462.
Xiong, Y., Xiao, T.F., Liu, Y.Z., Zhu, J.M., Ning, Z.P., Xiao, Q.X., 2017. Occurrence and mobility of toxic elements in coals from endemic fluorosis areas in the three gorges region SW China. Ecotoxicol. Environ. Saf. 144, 1–10.
Xu, M.H., Yan, R., Zheng, C.G., Qiao, Y., Han, J., Sheng, C.D., 2003. Status of trace element emission in a coal combustion process: a review. Fuel Process. Technol. 85, 215–237.
Xu, N., Braida, W., Christodoulatos, C., Chen, J.P., 2013. A review of molybdenum adsorption in soils/bed sediments: speciation, mechanism, and model applications. Soil Sediment Contam. 22 (8), 912–929.
Yang, J.P., Liu, D.Y., Wang, Y.J., Zhao, Y.C., Zhang, Y., Zhang, J.Y., Zheng, C.G., 2016. Rlease and the interaction mechanism of uranium and alkaline/alkaline-earth metals during coal combustion. Fuel 186, 405–413.
Yang, Y.H., Hu, H.Y., Xie, K., Huang, Y.D., Liu, H., Li, X., Yao, H., Ichiro, N., 2019. Insight of arsenic transformation behavior during high-arsenic coal combustion. Proc. Combust. Inst. 37 (4), 4443–4450.
Yao, L., Liao, H.P., Deng, C.Y., Yang, W., Lu, B., Li, T., 2012. Analysis of gains and losses of the ecosystem service function values of the three gorges region based on land use change – a case study of Wushan County in Chongqing. J. Southwest Univ. (Nat. Sci.). 34 (5), 91–96.
Yi, B.J., Zhang, L.Q., Huang, F., Xia, Z.J., Mao, Z.H., Ding, J.W., Zheng, C.G., 2015. Investigating the combustion characteristic temperature of 28 kinds of Chinese coal in oxy-fuel conditions. Energy Convers. Manag. 103, 439–447.
Yi, H., Hao, J., Lei, D., Tang, X., Ning, P., Li, X., 2008. Fine particle and trace element emissions from an anthracite coal-fired power plant equipped with a bag-house in China. Fuel 87 (10–11), 2050–2057.
Yu, J., Sun, L.S., Xiang, J., Hu, S., Su, S., Qiu, J.R., 2011. Vaporization of heavy metals during thermal treatment of model solid waste in a fluidized bed incinerator. Chemosphere 86 (11), 1122–1126.
Zeng, Q., Dong, J.X., Zhao, L.H., 2018. Investigation of the potential risk of coal fire to local environment: a case study of Daquanhu coal fire, Xinjiang region, China. Sci. Total Environ. 640, 1478–1488.
Zhang, J., Han, C.L., Xu, Y.Q., 2003. The release of the hazardous elements from coal in the initial stage of combustion process. Fuel Process. Technol. 84 (1–3), 121–133.
Zhao, S.L., Pudasainee, D., Duan, Y.F., Gupta, R., Liu, M., Lu, J.H., 2019. A review on mercury in coal combustion process: content and occurrence forms in coal, transformation, sampling methods, emission and control technologies. Prog. Energ. Combust. Sci. 73, 26–64.
Zhao, Y.C., Zhang, J.Y., Huang, W.C., Wang, Z.H., Li, Y., Song, D.Y., Zhao, F.H., Zheng, C. G., 2008. Arsenic emission during combustion of high arsenic coals from Southwestern Guizhou, China. Energy Convers. Manag. 49 (4), 615–624.
Zheng, B., Wu, D., Wang, B., Liu, X., Wang, M., Wang, A., Finkelman, R.B., 2007. Fluorosis caused by indoor coal combustion in China: discovery and progress. Environ. Geochem. Health 29 (2), 103–108.
Zheng, B.S., Wang, B.B., Ding, Z.H., Zhou, D.X., Zhou, Y.S., Zhou, C., Chen, C.C., Finkelman, R.B., 2005. Endemic arsenosis caused by indoor combustion of high-As Coal in Guizhou Province, PR China. Environ. Geochem. Health 27 (5), 521–528.
Zhou, C., Liu, G., Yan, Z., Fang, T., Wang, R., 2012. Transformation behavior of mineral composition and trace elements during coal gangue combustion. Fuel 97, 644–650.
Zhou, C., Liu, G., Xu, Z., Sun, H., Lam, P.K.S., 2017. The retention mechanism, transformation behavior and environmental implication of trace element during co-combustion coal gangue with soybean stalk. Fuel 189, 32–38.
Zhou, C.C., Liu, G.J., Fang, T., Lam, P.K.S., 2015. Investigation on thermal and trace element characteristics during co-combustion biomass with coal gangue. Bioresour. Technol. 175, 454–462.
Zhou, Q.R., Zhang, J., Chen, J., Xu, S.B., Yan, W., Guo, X.L., Yue, X.C., Zhao, J., Wang, Z. H., 2009. Analysis of the relationship between the urinary fluoeide and total fluoride intake in coal-burning fluorosis area in Chongqing. Mod. Prev. Med. 36 (20), 3833–3835.